

A Coupled ODR-DEM Method for Dispersion Fuel Analysis in RMC Code

Zhe Chuan Tan^{1,3}, Zhi Yuan Feng², Kok Yue Chan¹, Kan Wang¹

¹ *Department of Engineering Physics, Liu Qing Building, Tsinghua University, Beijing 100084, China;*

² *China Nuclear Power Engineering Co., Ltd, Beijing, 100840, China;*

³ *Department of Safety Analysis, Singapore Nuclear Research and Safety Initiative, Singapore 138602, Singapore*

ABSTRACT

Dispersion fuels exhibit excellent fuel performance and thermal conductivity, coupled with exceptional safety characteristics, leading to their widespread use in research and next generation reactors such as High Temperature Gas-Cooled Reactors and Pebble-Bed Reactors. However, the arrangement of densely packed dispersion fuel such as Fully Ceramic Micro-Encapsulated (FCM) fuel is stochastic in nature, resulting in geometric complexity that challenges existing geometric modeling methods implemented in Monte Carlo codes. In this paper, we introduce a coupling method for the Optimized Dropping and Rolling (ODR) method and the Discrete Element Method (DEM), two explicit modeling methods known for the precise and efficient geometric modeling of stochastic media. The aim of this paper is two-fold; firstly, to reduce the high computational expense commonly associated with DEM, and secondly, to remove the packing fraction upper limit commonly associated with the ODR method. The coupled ODR-DEM method was then verified against particle distributions generated via existing explicit modeling methods, and the results showed that the methods are able to generate stochastic medium that exceed the particle packing fraction limit seen by the ODR method. The method also showed significant time savings over the original DEM, showing that the pre-arrangement of particles via ODR is able to reduce computational expense by DEM by a considerable margin.

Keywords: Discrete Element Method; Optimized Dropping and Rolling Method; Stochastic Media; Dispersion Fuel; RMC

I. INTRODUCTION

The spatial arrangement and modeling of fuel particles in stochastic media is fundamental in many nuclear reactor simulations, particularly for micro fuel particles such as TRISO particles, where these fuels comprise of stochastic mixtures of spherical fuel and/or poison particles embedded within a matrix. This study is motivated by the resurgence of interest in dispersion fuels, driven by recent advancements in research and industrial applications of Fully Ceramic Microencapsulated (FCM) Fuels [1] [2] [3] [4] [5], and secondly, the demand for high fidelity dispersion fuel models for use in RMC code, a continuous-energy Reactor Monte Carlo neutron and photon transport code currently being developed by the Department of Engineering Physics at Tsinghua University, Beijing [6].

The ODR method [7] [8] is a robust explicit modeling method, with previous research showing that ODR can generate particle distributions at much higher computational efficiencies compared to other explicit methods such as the Classical Dropping and Rolling (CDR) method [7] and DEM [9]. However, as the ODR method assumes that all dropped particles remain static and immovable, ODR-generated particle distributions are typically less dense than those produced by DEM [9]. On the other hand, DEM is a dynamic simulation approach that models the physical interactions between individual particles. While it is most suited for modelling high particle packing fraction stochastic media, DEM is inherently computationally intensive and time-consuming [9] [10] [11], making it highly unfeasible for the simulation of complex, memory-intensive dispersion fuel systems.

As such, given the motivations cited above, this paper proposes a coupled ODR-DEM Method for high-particle packing fraction dispersion fuel modelling, with the goal of generating high packing fraction particle distributions above the density constraints of the ODR method, whilst being computationally efficient compared to DEM. To ensure that the paper is self-contained, we describe the methodology behind the ODR and DEM methods in Sections II.A and II.B respectively, and the

coupling method in Section II.C. Section III elaborates on the results of the coupled ODR-DEM method, and in Section IV, we summarize and conclude the paper, as well as discuss limitations and future work.

II. METHODOLOGY

II.A. The Optimized Dropping-Rolling Method

The ODR Method is described below. Certain steps are described briefly as the reader is directed to previous studies [7] [8] [12] for further elaboration and pictorial descriptions.

- 1) Step 0 (Initiating): A spherical particle is newly generated above the top boundary of the stochastic media, with its initial position as $S_1^0 = S(c_1^0, r_1)$, where c_1^0 is the particle center with coordinates (x_1^0, y_1^0, z_1^0) , and r_1 as the particle radius.
- 2) Step 1 (Dropping): Particles that may come into contact with the dropping particle are hence identified. The distance that the particle drops by just as it comes into first contact with either the bottom of the stochastic media, or other particles, is calculated. The particle position is then updated:

$$z_1^1 = z_2 + \sqrt{(r_1 + r_2)^2 - ((x_1^0 - x)^2 + (y_1^0 - y)^2)} \quad (1)$$

$$y_1^1 = y_1^0, x_1^1 = x_1^0 \quad (2)$$

$$S_1^1 = S(c_1^1(x_1^1, y_1^1, z_1^1), r_1) \quad (3)$$

- 3) Step 2 (Determining the Rolling Angle): The coordinates of c_1^1 are determined:

$$x_1^1 = x_2 + (r_1 + r_2)(\cos\varphi)(\cos\theta) \quad (4)$$

$$y_1^1 = y_2 + (r_1 + r_2)(\cos\varphi)(\sin\theta) \quad (5)$$

$$z_1^1 = z_2 + (r_1 + r_2)(\sin\varphi) \quad (6)$$

where θ is the azimuthal angle, and φ is the polar angle. The unique pair of angles ($\theta \in [0, 2\pi]$, $\varphi \in [0, \pi/2]$) is determined by the governing equations 4, 5, and 6. The new working basis $B_0 = (u_0, v_0, w_0)$ is established by applying a rotation defined by angle θ . The matrix that transforms coordinates from the canonical basis (x, y, z) to the rotated basis B_0 is denoted as M_0 .

- 4) Step 3 (Rolling Phase 1): As described in Hitti and Bernacki [7], the initial step involves identifying the particles that intersect with the torus defined by the axis, a minor radius r_1 , and a major radius of $(r_1 + r_2)$. If no particles intersect the torus, the updated coordinates of c_1^1 are computed by setting $\varphi = 0$ in Eq. 4, 5, and 6. In this case, the algorithm reverts to the initial dropping step, where $S_1^0 = S_1^1$. However, if particles are found to intersect the torus, the method proceeds to identify a particle S_3 for which the angle φ' is maximized, with $\varphi' \in [0, \varphi]$. By setting $T = \cos\varphi'$, the valid values of T correspond to the roots of the following:

$$(K_1^2 + K_2^2)T^2 - 2K_1K_3T + K_3^2 - K_2^2 = 0 \quad (7)$$

$$K_2(K_3 - K_1T_i) \geq 0 \quad (8)$$

where $K_1 = 2(W_x \cos\theta + W_y \sin\theta)$, $K_2 = 2W_z$, $K_3 = (W_x^2 + W_y^2 + W_z^2 + 1 - W^2)$, and the values of W correspond to $W_x = \frac{x - x_2}{r_1 + r_2}$, $W_y = \frac{y - y_2}{r_1 + r_2}$, $W_z = \frac{z - z_2}{r_1 + r_2}$, $W = \frac{r + r_1}{r_1 + r_2}$

- 5) Step 4 (Surface Intersection Check 1): The particle is then checked for intersection with the boundaries of the dispersion fuel, as per Hitti and Bernacki [7]. However, for a cylindrical annulus, the governing equations are slightly different, as per Feng et al [8]. If the particle drops below the lower surface, we compute φ'_{new} and reposition the particle so it touches the surface.
- 6) Step 5 (Local Coordinate System Transformation): Prior to the interaction of two colliding particles, a new coordinate system (Ω, B_1) must be established based on the rolling angle β . For more information on constructing this coordinate system, refer to Hitti and Bernacki [7] and Feng et al [8] [12]. In this local coordinate system, the position of c_1^2 is expressed as $(0; \Omega c_1^2 \cdot \cos\beta; \Omega c_1^2 \cdot \sin\beta)$
- 7) Step 6 (Rolling Phase 2): As per Step 3, we identify particles that intersect the torus defined by the axis c_2c_3 , centered at Ωc_1^2 , with a small radius (r_1) and a large radius Ωc_1^2 . If no particle intersects the torus, we assign $\beta = \pi$, update the particle's position, and then check the new position of the dropping particle. If $z_1^3 \leq \min(z_2, z_3)$, we return to Step 1, setting $S_1^0 = S_1^3$. In other cases, we must consider a condition not accounted for in Hitti and Bernacki's study [7]: if $z_3 < z_1^3$ or $z_2 < z_1^3$, we revert to Step 2, replacing S_2 with S_3 . If any particle does intersect the torus, we thus search for the particle associated with the smallest verified rolling angle β' in the (Ω, B_1) coordinate system, indicating that this particle is the first contacted particle along the dropping particle's rolling process, where β' is defined as:

$$\text{If } \beta < 0, \beta' \in [-\pi, \beta]; \quad (9)$$

$$\text{Else if } \beta \geq 0, \beta' \in [\beta, \pi]; \quad (10)$$

The coordinates of the particle in the transformed basis are also obtained per Eq. 11. By setting $T = \cos\beta'$, the values of T that solve the system are thus the roots of the quadratic equation in Eq. 7 and 8.

$$\vec{x}_1^3 = 0, \vec{y}_1^3 = \Omega c_1^2 \cdot \cos \beta', \vec{z}_1^3 = \Omega c_1^2 \cdot \sin \beta' \quad (11)$$

- 8) Step 7 (Surface Intersection Check 2): The dropping particle is again checked for intersections with other particles and boundary surfaces, following the process in Step 4.
- 9) Step 8 (Stability Check): To check the stability of the dropped particle, we utilize the classical test, with the projection of the particle centers of the contacting particles onto the horizontal plane being considered. The reader is referred to previous work by Hitti and Bernacki [7] for the calculation process.

The ODR Method is highly efficient, working on the assumption that all other particles remain static during the dropping process, and neglecting particle dynamics. The utilization of a direct rolling system, although fast, results in the ODR method suffering from a lower saturation limit compared to other methods such as DEM, making the particle distributions produced by ODR much less realistic than these other methods.

II.B. The Discrete Element Method

The Discrete Element Method (DEM) simulates particle behavior in granular flows by explicitly modeling particle-particle interactions governed by Newtonian mechanics [13], where particle contacts and individual particle motions acting on each particle are considered. Newton's Second Law is used to determine the net displacement of each particle resulting from the cumulative contact forces acting on it, while a force-displacement law is applied to determine the contact forces arising from interactions with other particles or the boundaries of the stochastic medium. To determine the forces acting on the particle, normal overlap and tangential motion is considered during calculations. The dampened linear spring contact force model as discussed in Cundall and Strack [13] is utilized to derive the normal and tangential forces acting upon the particle:

$$F_{nij} = (-k_n \alpha^{3/2} - c_n \vec{v}_{ij} \cdot \vec{n}) \quad (12)$$

$$F_{tij} = (-k_t \delta - c_t \vec{v}_{ct}) \quad (13)$$

Where F_{nij} and F_{tij} are the normal and tangential forces acting on the particle respectively; α represents the overlap distance between particles; δ is the tangential overlap displacement; k_n and k_t denote the linear spring stiffness in the normal and tangential directions; \vec{v}_{ij} is the relative velocity of the interacting particles; and c_n and c_t are the dashpot coefficients in the normal and tangential directions, respectively.

As DEM considers particle dynamics, it is able to produce highly realistic and accurate particle distributions. However, DEM is highly computational expensive, especially in simulations involving large numbers of particles. Hence, there is motivation to reduce the high computational cost associated with DEM.

II.C. The Coupled ODR-DEM Method

The coupled ODR-DEM method is described in Fig. 1. ODR is used primarily to place particles within stochastic media in a “pre-arrangement” process. Afterwards, DEM is applied to simulate particle dynamics, while random forces are applied to the particles to simulate shaking processes, similar to that of existing manufacturing methods in FCM fuel. The post-DEM fuel is thus able to achieve packing fractions above the saturation limit of ODR, whilst having a reduced computational expense due to the application of ODR to place all particles prior to DEM.

III. RESULTS AND DISCUSSION

The algorithm was implemented as a function within RMC code, and was executed on an AMD Ryzen Threadripper 3990X 64-Core Processor, utilizing only a single thread for all computations. For each calculation set, 100 independent runs were performed, and the averaged result of these runs was used for comparison. In Section III.A, we discuss the performance of the coupled ODR-DEM method with respect to the saturation limit of the generated particle distributions. Section III.B discusses the effectiveness of the coupled ODR-DEM method with respect to computational expense and accuracy. In Section III.C, we discuss limitations and future work.

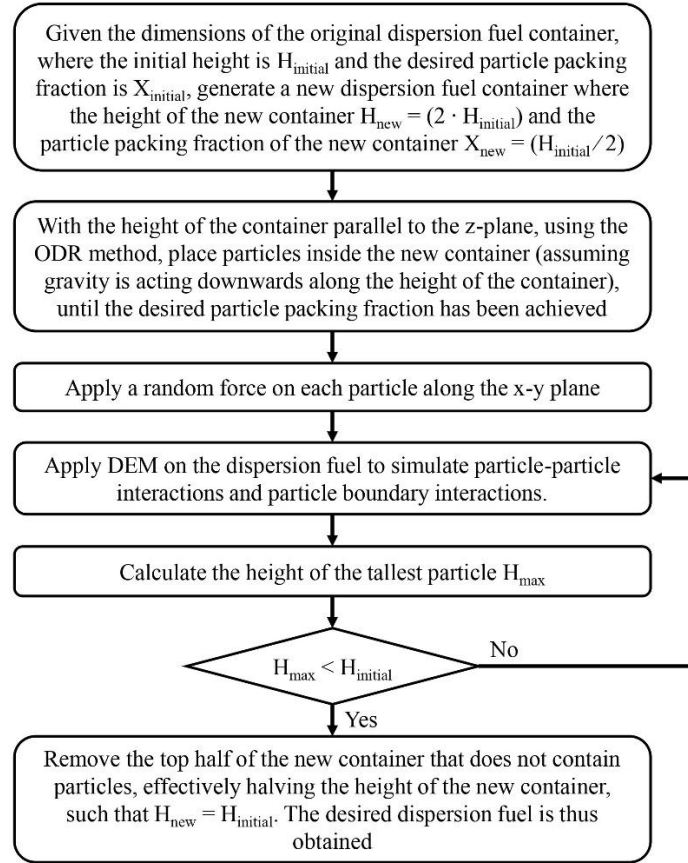


FIGURE 1. The Coupled ODR-DEM Method

III.A. Evaluation of Upper Particle Packing Fraction Limit of the Coupled ODR-DEM Method

In this Section, we utilized a cuboidal stochastic medium filled with mono-spheres as described in Hitti and Bernacki [7], and compared the results against the ODR and DEM methods respectively. Table I described the test parameters, whilst Table II displays the results for the saturation limit comparison.

TABLE I. Stochastic Medium Parameters

Parameter	Value (cm)
Length	30.0
Width	30.0
Height	35.0
Particle Radius	1.0

TABLE II. Saturation Limit Comparison between Different Geometry Modeling Methods in RMC

Method	Saturation Limit	Standard Deviation
Optimized Dropping and Rolling Method	0.576	0.0008
Discrete Element Method	0.638	0.0009
Coupled ODR-DEM Method	0.638	0.0011

The testing results from the ODR and DEM methods agree with those from current literature [7] [14]. Moreover, it can be observed that the coupled ODR-DEM Method is able to produce particle distributions that exceed the saturation limit of ODR, similar to those of DEM.

III.B. Evaluation of Upper Particle Packing Fraction Limit of the Coupled ODR-DEM Method

In this section, we compare the modelling methods in terms of stochastic media generation time and k_{inf} values between DEM and the coupled ODR-DEM Method. Tables III and IV describe the dispersion fuel parameters and fuel particle parameters respectively. In particular, in Table IV, **Layer** refers to the current layer of the particle, starting from the innermost layer of the fuel kernel, and **Rad** refers to the overall particle radius. **Rad** was varied between 0.150 and 0.350, and the particle packing fraction was set to 0.40. The results are shown in Tables V and VI, where the stochastic media generation time and k_{inf} values are compared respectively.

TABLE III. Dispersion Fuel Parameters

Parameter	Value
Boundary Condition	Full Reflection
Radius	9.00 (cm)
Height	40.00 (cm)
Matrix Material	Graphite

TABLE IV. Particle Parameters for k_{inf} Comparison

Layer	Radius/cm	Density/g/cm ³	Material
Fuel Kernel	(Rad - 0.085)	12.95	UC
Layer 1	(Rad - 0.035)	1.050	C
Layer 2	(Rad - 0.015)	1.900	C
Layer 3	(Rad - 0.005)	3.160	SiC
Layer 4	Rad	1.100	C

TABLE V. Stochastic Media Generation Time Comparison between Original DEM and Coupled ODR-DEM Method

Particle Radius (cm)	Stochastic Media Generation Time (seconds)		
	DEM	Coupled ODR-DEM	Factor
0.350	26.357	0.17017	154.88
0.300	69.782	0.50017	139.52
0.250	130.40	0.81112	160.77
0.200	345.32	2.30892	149.56
0.150	1443.8	9.58053	150.70

TABLE VI. k_{inf} Comparison between Original DEM and Coupled ODR-DEM Method

Particle Radius (cm)	Stochastic Media Generation Time (seconds)	
	DEM	Coupled ODR-DEM
0.350	1.000958 ± 0.000689	1.001195 ± 0.000648
0.300	1.001491 ± 0.000596	1.001733 ± 0.000718
0.250	1.002105 ± 0.000639	1.001638 ± 0.000597
0.200	1.001859 ± 0.000622	1.002295 ± 0.000712
0.150	1.000849 ± 0.000590	1.001501 ± 0.000691

As shown in Table V, the couple ODR-DEM Method generates particle distributions with a much reduced generation time, with the reduction in computational time by a factor of more than 100 across all particle radii. Furthermore, we can observe in Table VI that for all particle radii, the values of k_{inf} between the original DEM and coupled ODR-DEM methods are within three standard deviations of each other. It must be noted that as the particle distributions change, the k_{inf} will naturally change, hence the k_{inf} values cannot be directly compared with each other. However, this is a good gauge of how both processes are able to produce similar particle distributions with similar k_{inf} values. Hence, we can see that the coupled ODR-DEM method has achieved its objective of developing particle generations above the saturation limit of ODR, whilst being computationally effective against DEM.

III.C. Limitations and Future Work

There are inherent limitations to the results presented in this paper. Firstly, the computational time reported is solely the stochastic media generation time, which does not include processes that are typically considered in the total simulation time, such as inactive and active cycle calculations and burnup cycles. As the total simulation time is highly dependent on other factors, the proportion of the total simulation time that is spent on stochastic media generation may be much smaller than the time spent on other processes. Secondly, it can be observed that the ODR method is mainly used in simulating spherical particles, and as such, the coupled ODR-DEM method is limited only to spheres in this paper. This remains a potential area for improvement and research.

Regarding future work, there are a few improvements that we believe can be considered. The main mechanism within the coupled ODR-DEM method, where particles are placed via ODR and DEM is used to simulate particle shaking and settling, can be iterated for an even greater reduction in computational time. For instance, the configuration of the stochastic media may be maintained, and particles then added in via ODR. DEM is then applied to simulate particle dynamics, and the “settled” particles can then be “fixed” in space, so that future DEM processes will no longer consider particle dynamics for these “settled” portions of the stochastic media, hence reducing computational expense further. In the empty space that appears after the particles have been settled, ODR can then be used to place more particles, and this iterates until the required packing fraction is achieved. This method is algorithmically more complex, but it should promise even greater time savings.

IV. CONCLUSIONS

The ODR and DEM methods are well-established and extensively studied explicit modeling approaches, yet each comes with inherent limitations. Specifically, the ODR method does not account for particle dynamics and has a low saturation limit, while DEM is computationally intensive. To address these shortcomings, this work introduces the coupled ODR-DEM methods, designed to efficiently generate high packing fraction particle distributions that surpass the density limitations of ODR alone. The coupled ODR-DEM method successfully achieved packing densities beyond the ODR’s upper threshold, comparable to those produced by DEM.

Moreover, when evaluated with variable particle radii, the coupled ODR-DEM method demonstrated significantly higher computational efficiency than DEM, while still producing particle arrangements with similar randomness and k_{inf} values—preserving both accuracy and reliability. As such, we consider this approach to be a valuable advancement in the modeling and simulation of dispersion fuel microstructures. Additionally, it holds potential for broader application in fields that rely on DEM, including granular flow and stochastic media containing non-spherical particles.

ACKNOWLEDGMENTS

This work is supported by the Department of Engineering Physics, Tsinghua University, where the use of High Performance Computing resources was supported.

REFERENCES

- [1] Zaidabadi MZ, Ansarifa GR. Design of a small modular nuclear reactor with dual cooled annular fuel and investigation of the fuel inner radius effect on the power peaking factor and natural circulation parameters. *Annals of Nuclear Energy*. 2020 Apr;138:107185.
- [2] Wang M, Zhou B, Bu S, Li Z, Chen D, Ma Z, Zhang L. A multi-annulus heat conduction model for predicting the peak temperature of nuclear fuels with randomly dispersed TRISO particles. *Progress in Nuclear Energy*. 2023 Apr;158:104602.
- [3] Rabir MH, Ismail AF, Yahya MS. Neutronics calculation of the conceptual TRISO duplex fuel rod design. *Nuclear Materials and Energy*. 2021 Jun;27:101005.
- [4] Ivanusa P, Jensen P, Condon CA, Bunn AL. Comparison of irradiated TRISO fuel radioactivity from multiple advanced reactor designs. *Nuclear Technology*. 2021 Sep;208:575–585.
- [5] Choi JY, Hong SG, Kwon H. Conceptual design of a long cycle small modular reactor core with annular UO₂ and FCM (TRU) fuels. *International Journal of Energy Research*. 2020 Sep; 45:11957–11975.
- [6] Wang K, Li Z, She D, Liang J, Xu Q, Qiu Y, Yu J, Sun J, Fan X, Yu G. RMC - a Monte Carlo code for reactor core analysis. *SNA + MC 2013 - Joint International Conference on Supercomputing in Nuclear Applications + Monte Carlo*. 2014;06020.
- [7] Hitti K, Bernacki M. Optimized dropping and rolling (ODR) method for packing of polydisperse spheres. *Applied Mathematical Modelling*. 2013 Apr;37:5715–5722.

- [8] Feng Z, Liang J, Guo W, Wang K. Optimized dropping and rolling and virtual surface method for high packing fraction of dispersed fuel particles in annular container. *Nuclear Science and Engineering*. 2024 Sep;1–9.
- [9] Feng Z, An N, Wang K. An improved distinct element method for high packing fraction stochastic media modeling. *EPJ Web of Conferences*. 2021;247:04026.
- [10] Jajcevic D, Siegmann E, Radeke C, Khinast JG. Large-scale CFD–dem simulations of fluidized granular systems. *Chemical Engineering Science*. 2013 Jul;98:298–310.
- [11] Berger KJ, Hrenya CM. Challenges of DEM: II. wide particle size distributions. *PowderTechnology*. 2014 Sep;264:627–633.
- [12] Feng Z, An N, Liang J, Wang K. ODR-vs method for a high packing fraction of dispersed TRISO particles. *Annals of Nuclear Energy*. 2022 Feb;166:108821.
- [13] Cundall PA, Strack OD. Discussion: A discrete numerical model for granular assemblies. *Géotechnique*. 1980 Sep;30:331–336.
- [14] Dai L, Sorkin V, Vastola G, Zhang YW. Dynamics calibration of particle sandpile packing characteristics via discrete element method. *Powder Technology*. 2019 Apr;347:220–226.